C_s-Symmetric *ansa*-Lanthanocenes Designed for Stereospecific Polymerization of Methyl Methacrylate. Synthesis and Structural Characterization of Silylene-Bridged Fluorenyl Cyclopentadienyl Lanthanide Halides, Amides, and Hydrocarbyls

Changtao Qian,* Wanli Nie, and Jie Sun

Laboratory of Organometallic Chemistry, Shanghai Institute of Organic Chemistry,
Chinese Academy Of Sciences, 354 Fenglin Lu, Shanghai 200032, China

Received March 30, 2000

A series of new C_s-symmetric organolanthanocene chlorides, $[R_2Si(Flu)(R'Cp)Ln(\mu\text{-}Cl)]_2$ (Flu = $C_{13}H_8$, fluorenyl; Cp = C_5H_3) (R = Me, R′ = H, Ln = Y (**1**), Lu (**2**), Dy (**3**), Er (**4**); R = Ph, R′ = ^tBu, Ln = Y (**5**), Dy (**6**)), has been synthesized by the reaction of anhydrous lanthanide chloride with the dilithium salt of the ligand $Me_2Si(FluH)(CpH)$. Treatment of the resulting chlorides with $ME(TMS)_2$ (M = Li or K, E = N, CH) gave the amide and hydrocarbyl derivatives $Me_2Si(Flu)(Cp)LnE(TMS)_2$ (E = N, Ln = Dy (**7**), Er (**9**); E = CH, Ln = Dy (**8**), Er (**10**)). X-ray structures of chloride compounds reveal unusual Cp−$SiMe_2$−Cp bridging dimeric coordination. All of the amide and hydrocarbyl complexes show normal chelating structure and exhibit apparently intramolecular γ-agostic Ln−Me−Si interaction. These complexes are active for the polymerization of methyl methacrylate.

Introduction

In the past few decades, stereorigid early transition and lanthanide element metallocenes have been established as excellent catalysts or precatalysts for the stereospecific polymerization of propylene and other α-olefins. Especially exciting are the prospects for tailoring the polymer microstructure by systematic, rational variation of the substituents of the two cyclopentadienyl ligands, particularly when they are connected by an interannuler bridge.[1] Thus, these “*ansa*”-metallocene derivatives have been the subject of this study, following the pioneering work by Brintzinger and co-workers.[2] Organometallic complexes containing two cyclopentadienyl or tetramethylcyclopentadienyl ligands bridged by Me_2Si or Et_2Si uints have been widely empolyed in the synthesis of a variety of *ansa*-metallocenes including zirconium[3] and lanthanide metals.[4]

More recently rare-earth metal complexes were found to initiate living polymerization of polar and nonpolar monomers and allow the synthesis of high molecular weight polymers with extremely narrow molecular weight distributions. Yasuda’s and Marks’s groups have studied the activity of the C_{2v}- and C_1-symmetric organolanthanocene complexes for the polymerization of methyl methacrylate (MMA).[5,6] In our previous work we have reported the synthesis and characterization of the CPh_2-bridged C_s-symmetric complexes of lanthanocene chloride and borohydride.[7] Yasuda et al. reported the catalysis of Me_2Si-bridged C_s-symmetric rare-earth Ln(III)[8] and Ln(II)[9] complexes for polymerization of ethylene and α-olefin. As an extension of the ligand modification for lanthanide complexes, we attempted to report new type of C_s-symmetric silyene-bridged fluorenyl cyclopentadienyl organolanthanide halide, amide, and hydrocarbyl complexes to investigate the relation between the structures of rare-earth metal complexes and their activity toward MMA.

Results and Discussion

Synthesis. These chloride, hydrocarbyl, and amide complexes were synthesized as described in Scheme 1.

---

* Corresponding author. E-mail: qianct@pub.sioc.ac.cn. Fax: 0086-21-64166128.

(1) (a) Kaminsky, W.; Kulper, K.; Brintzinger H. H.; Wild, F. R. W. P. *Angew. Chem., Int. Ed. Engl.* **1985**, *24*, 507. (b) Ewen, J. A.; Jones R. L.; Razavi, A. *J. Am. Chem. Soc.* **1988**, *110*, 6255. (c) Piccolrovazzi, N.; Pino, P.; Consiglio, G.; Sironi A.; Moret, M. *Organometallics* **1990**, *9*, 3098. (d) Ewen, J. A.; Haspeslagh, L.; Atwood J. L.; Zhang, H. *J. Am. Chem. Soc.* **1987**, *109*, 6544. (e) Rieger, B. *J. Organomet. Chem.* **1982**, *428*, C23. (f) Okuda, J. *Angew. Chem., Int. Ed. Engl.* **1992**, *31*, 47. (g) Razavi A.; Atwood, J. L. *J. Organomet. Chem.* **1993**, *459*, 117.

(2) Smikth, J. A.; Von Seyerl, J.; Hattner, G.; Brintzinger, H. H. *J. Organomet. Chem.* **1979**, *173*, 175.

(3) (a) Batgur, C. S.; Tikkanen W. R.; Peterson, J. L. *Inorg. Chem.* **1985**, *24*, 2539. (b) Jutzi, P.; Dickbreder, R. *Chem. Ber.* **1986**, *119*, 1750.

(4) (a) Haar, C. M.; Stern C. L.; Marks, T. J. *Organometallics* **1996**, *15*, 1765. (b) Coughlin, E. B.; Henling, L. M.; Bercaw, J. E. *Inorg. Chim. Acta* **1996**, *242*, 205. (c) Giardello, M. A.; Sabat, M.; Rheingold, A. L.; Stern, C. L. *J. Am. Chem. Soc.* **1994**, *116*, 10212. (d) Qaio, K.; Fisher R. D.; Paolucci, G. *J. Organomet. Chem.* **1993**, *456*, 185. (e) Akhnoukh, T.; Muller, J.; Qiao, K.; Li, X.-F.; Fischer, R. D. *J. Organomet. Chem.* **1991**, *408*, 47. (f) Stern, D.; Sabat, M.; Marks, T. J. *J. Am. Chem. Soc.* **1990**, *112*, 9558. (g) Heeres, H. J.; Renkema, J.; Meetrsma, A.; Teuben, J. H. *Organometallics* **1988**, *7*, 2495.

(5) (a) Yasuda, H.; Ihara, E. *Bull. Chem. Soc. Jpn.* **1997**, *70*, 1745. (b) Yasuda, H.; Yamamoto, H.; Yamashita, M.; Yokota, K.; Nakamura, A.; Miyake, S.; Kai, Y.; Kanehisa, N. *Macromolecules* **1993**, *26*, 7134. (c) Yasuda, H.; Tamai, H. *Prog. Polym. Sci.* **1993**, *18*, 1097.

(6) Giardello, M. A.; Yamamota, Y.; Bard, L.; Marks, T. J. *J. Am. Chem. Soc.* **1995**, *117*, 327.

(7) Qian, C.; Nie W.; Sun, J. *J. Chem. Soc., Dalton Trans.* **1999**, 3283.

(8) (a) Yasuda, H.; Ihara, E. *Adv. Polym. Sci.* **1997**, *133*, 53. (b) Yasuda, H.; Ihara, E.; Nitto, Y.; Kakehi, T.; Morimoto, M.; Nodono, M. *ACS Symp. Ser.* **1998**, *704*, 149.

(9) Ihara, E.; Nodono, M.; Katsura, K.; Adachi, Y.; Yasuda, H.; Yamagashira, M.; Hashimoto, H.; Kanehisa, N.; Kai, Y. *Organometallics* **1998**, *17*, 3945.

10.1021/om000276f CCC: $19.00
Publication on Web 09/07/2000

Scheme 1

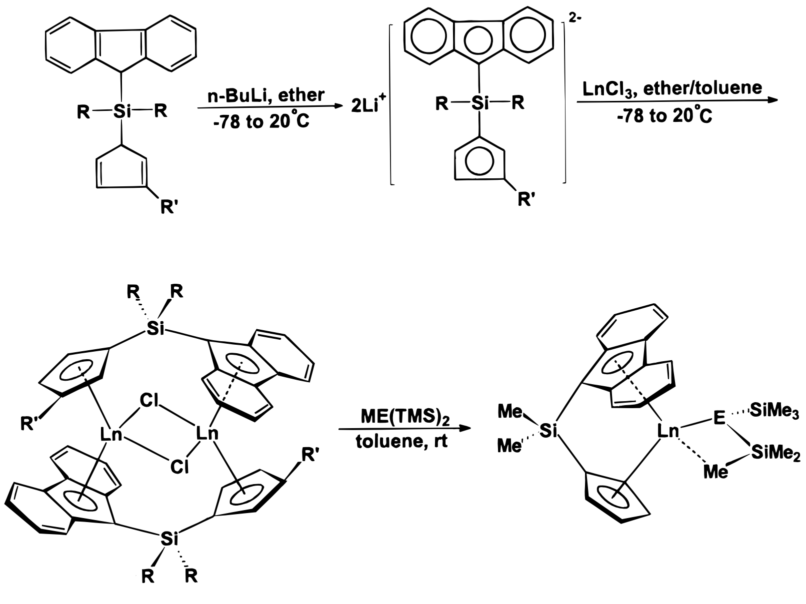

R=Me, R'=H; Ln = Y (**1**), Lu (**2**), Er (**3**), Dy (**4**) Ln=Dy; E=N (**7**), CH (**8**)

R=Ph, R'=t-Bu; Ln=Y (**5**), Dy (**6**) Ln=Er; E=N (**9**), CH (**10**)

By reaction of the dilithio salt of the ligands [$Me_2Si(C_5H_5)(C_{13}H_9)$][10] with anhydrous lanthanide chloride we got the solvent-free dimeric chlorides [$Me_2Si(C_5H_4)(C_{13}H_8)LnCl$]$_2$ (Ln = Y (**1**), Lu (**2**), Er (**3**), Dy (**4**)). The X-ray crystal structures indicated that all of the complexes assume the Cp−SiMe$_2$−Cp bridging structure instead of the normal chelating structure. Organometallic complexes containing two cyclopentadienyl or two tetramethylcyclopentadienyl ligands bridged by silylene units are genarally known to asssume the metal-chelating structure,[11] although only a rare example of bridging structure is already reported.[12] It still remains unclear whether dialkylsilyene-linked biscyclopentadienyl derivatives generally would be more stable as the chelating or bridging isomer. To understand the effect of different substituents on the coordination modes, we synthesized solvent-free dimeric chlorides [$Ph_2Si(^tBu\text{-}C_5H_3)(C_{13}H_8)$ LnCl]$_2$ (Ln = Y (**5**), Dy (**6**)). X-ray analysis revealed the existence of the C_1-symmetric complex as a bridging structure. This fact indicated that the bulkier substituents on the Cp ring and on the silylene-bridged atom did not hamper the formation of the bridging structure.

Since the less sterically demanding *ansa*-ligands promote the binding of additional ligands to the central equatorial site, the eletrophilicity of the metal increased. Consistent with this notion, the chlorides of [$R_2Si(C_5H_3R')(C_{13}H_8)LnCl$]$_2$ (**1**−**6**) exist as dimeric structures in the solid state.

The monomeric salt-free and solvent-free amido and hydrocarbyl complexes [$Me_2Si(C_5H_4)(C_{13}H_8)$]LnE(TMS)$_2$ (E = N, Ln = Dy (**7**), Er (**9**); E = CH, Ln = Dy (**8**), Er (**10**)) were synthesized by reaction of anhydrous $LnCl_3$ with the dilithio salt of the silylene-bridged ligand in ether, followed by the treatment with ME(TMS)$_2$ (M = K or Li; E = N, CH) in toluene in a one-pot procedure. The X-ray crystal structures displayed γ-agostic interactions between the M and methyl group in all of the amido and hydrocarbyl complexes.

The lanthanocene chlorides are readily dissolved in THF and ether and just sparing soluble in toluene at room temperature, but the amide and hydrocarbyl complexes are very soluble in toluene and benzene and sparingly soluble in hexane. All complexes remain air and moisture sensitive, whether in both solid and solution phases. Structures were confirmed by EA, MS, FT-Raman, or X-ray crystal analysis.

Mass Spectrometric Study of these Binuclear Organolanthanide Chlorides. It was known that the ligands [$MeSi_2(C_5R_4)_2$]$^{2-}$ (DMCS) (R = H, Me) should bond to early d-transition, lanthanide, and actinide metals to afford two different isomeric forms, I (chelating) and II (bridging) (Scheme 2), of the general type [$MeSi_2(C_5R_4)_2M(\mu\text{-}Cl)$]$_2$. In 1990, R. Dieter Fischer[13] demonstrated that mass spectrometry is a very powerful and versatile tool to identify the specific type of isomer in organolanthanide chemistry. He pointed out that the complex exists as the isomeric form II corresponding with almost exclusive binuclear fragments in the original mass spectra, while the predominance of mononuclear fragments might suggest the presence of a chloride bridge, which only existed in isomer I. However it can be seen from the Table 1 that complexes **1**−**6** show relatively low signals of binuclear fragments (M, M−Cl,

---

[10] (a) Patsidis, K.; Alt, H. G.; Milius, W.; Palackal, S. J. *J. Organomet. Chem.* **1996**, *509*, 63. (b) Chen, Y.; Rausch, M. D.; Chien, J. C. W. *J. Organomet. Chem.* **1995**, *497*, 1.

[11] (a) Abriel, W.; Heck, J. *J. Organomet. Chem.* **1986**, *302*, 363. (b) Jeske, G.; Schock, L. E.; Swepston, P. N.; Schumann, H.; Marks, T. J. *J. Am. Chem. Soc.* **1985**, *107*, 8103. (c) Fendrick, C. M.; Mintz, E. A.; Schertz, L. D.; Marks, T. J.; Day, V. W. *Organometallics* **1984**, *3*, 819.

[12] Hock, N.; Oroschin, W.; Paolucci, G.; Fisher, R. D. *Angew. Chem., Int. Ed. Engl.* **1986**, *25*, 5**,** 738**.**

[13] Qiao, K.; Fischer, R. D. *Organometallics* **1990**, *9*, 1361.

Table 1. Mass Spectrometric Results of the Chloride Complexes

fragment (%)	$[M]^+$	$[M - LnCl_2]^+$	$[M - LnCl_2{-}Flu]^+$	$[M/2]^+$	$[M/2 - Cl]^+$
1	820(5.54)	663(3.64)	497(12.35)	410(100)	374(40.25)
2	992(16.71)	749(2.21)	583(4.65)	496(100)	461(32.66)
3	974(14.17)	743(8.31)	575(18.56)	487(81.06)	453(100)
4	970(1.00)	738	572	485(2.35)	450(2.21)
5					554(0.32)
6		1099(4.23)		665(60.89)	630(17.59)

Table 2. X-ray Diffraction Data Collection Parameters for Complexes 1, 5, 7, 8, and 9

	1	**5**	**7**	**8**	**9**
formula	$C_{54}H_{52}Si_2Cl_2Y_2$	$C_{74}H_{66}Si_2Cl_2Y_2$	$C_{26}H_{36}Si_3NDy$	$C_{27}H_{37}Si_3Dy$	$C_{26}H_{36}Si_3NEr$
fw	1005.89	1260.22	609.33	608.35	614.09
cryst syst	triclinic	monoclinic	monoclinic	monoclinic	monoclinic
space group	$P\bar{1}$	$C2/c$	$P2_1/n$	$P2_1/n$	$P2_1/n$
a, Å	11.669(2)	25.996(4)	9.123(1)	13.759(2)	9.097(4)
b, Å	11.947(3)	10.008(2)	11.843(9)	9.077(9)	11.759(4)
c, Å	9.286(2)	24.261(3)	25.522(4)	45.18(1)	25.664(5)
α, deg	100.91(2)				
β, deg	100.00(1)	96.27(1)	93.47(1)	91.06(2)	93.41(3)
γ, deg	72.22(2)				
V, Å^3	1201.2(5)	6274(1)	2752.4(6)	5642(1)	2740(1)
Z	1	4	4	8	4
D_{calcd}, Mg/m^3	1.390	1.334	1.470	1.432	1.488
F(000)	516.00	2600.00	1228.00	2456.00	1236.00
μ, cm^{-1}	26.03	20.08	28.63	27.919	32.01
no. reflns	4249	5958	4407	9901	5420
no. observations	3028	3652	3357	7315	4046
no. variables	225	349	281	559	281
final *R*, R_w^{a}	0.051; 0.064	0.051; 0.065	0.034; 0.053	0.052; 0.066	0.030; 0.039
peak, hole/e Å^3	1.22; −0.64	1.01; −0.69	0.99; −0.90	1.49; −1.35	1832; −1.60

^{a} $R = \Sigma||F_o| - |F_c||/\Sigma|F_o|$, $R_w = [\Sigma w(|F_o| - |F_c|)^2/\Sigma|F_o|2]^{0.5}$.

Scheme 2

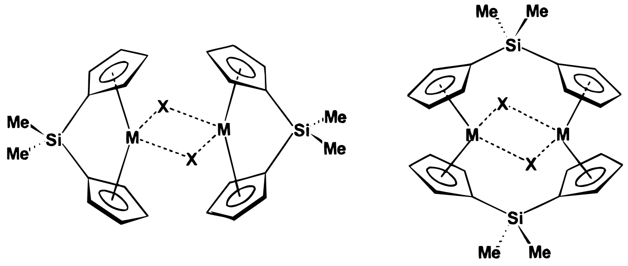

I II

M−LnCl, M−LnCl−Flu) and strong signals for mononuclear fragments (M/2, M/2−Cl, M/2−Cl−Me). This result is not consistent with the conclusion made by D. Fischer. This is perhaps due to different structures between the two chloride systems.

Molecular Structures. Crystals of **1**, **5**, **7**, **8**, and **9** were grown from toluene/*n*-hexane solution. Details of the crystal data and refinements are shown in Table 2, and selected bond lengths and internal angles in Tables 3−5, respectively. X-ray crystal structures of **1**, **5**, **7**, and **8** are shown in Figures 1−4, respectively.

In the crystal structure of complex **1**, the Y_2Cl_2 skeleton is almost a square. The angles of Cl−Y−Cl′ and Y−Cl−Y′ are 88.18° and 91.82°, respectively. The Y−Y′ distance of 3.797 Å is shorter than that of 3.987 Å in the cheleting isomer I of $[(C_5H_5)_2Yb(\mu\text{-}Cl)]_2$,[14] while it compare well with that of 3.750 Å for the bridging isomer $[Me_2Si(C_5H_4)_2Yb(\mu\text{-}Cl)]_2$[12] (ionic radius of Y^{3+} is only 0.03 Å larger than that of Yb^{3+}). In the C_1 complex the Y_2Cl_2 skeleton is somewhat different from that of C_s-symmetric compounds. It has a rhombic arrangement. The angles Cl−Y−Cl′ and Y−Cl−Y′ are 88.0° and 102.4°, respectively. The Y−Y′ distance of 3.659 Å is shorter than that of 3.797 Å in the analogues C_s-symmetric complex **1**. In these binuclear complexes the Y−Cl (2.645 Å) for **1** and 2.641 Å for **5** are somewhat longer than that in the mononuclear complexes (e.g., for 2.610 Å in $Me_2Si(Flu)(Cp^*)YCl_2Li(Et_2O)_2$ ($Cp^* = C_5Me_4$)[15] and for 2.627 Å in $Me_2Si[(SiMe_3Cp)(CMe_3Cp)]YCl_2LiEt_2O$[16]).

Table 3. Selected Angles and Bonds for Complexes 1 and 5

	1	**5**
Bond Lengths (Å)		
Y−Y′	3.797(8)	3.659(1)
Y−Cl	2.649(2)	2.633(2)
Y−Cl′	2.638(2)	2.348(4)
Y−C(1)	2.601(6)	2.604(6)
Y−C(2)	2.580(8)	2.645(6)
Y−C(3)	2.599(8)	2.702(6)
Y−C(4)	2.623(7)	2.645(6)
Y−C(5)	2.635(5)	2.648(5)
Y−C(6)	2.601(5)	2.645(5)
Y−C(7)	2.681(6)	2.632(6)
Y−C(8)	2.699(6)	2.732(6)
Y−C(9)	2.651(6)	2.825(6)
Y−C(10)	2.599(6)	2.745(5)
Bond Angles (deg)		
Y−Cl−Y′	91.82(6)	88.0(1)
Cl−Y−Cl′	88.18(6)	102.4(3)
C(5)−Si−C(6)	118.1(2)	116.1(2)
C(20)−Si−C(19)	107.9(4)	106.9(3)
Dihedral Angle (deg)		
planes (1) and (2)	137.62	139.65

---

(14) Lueken, H.; Schmitz, J.; Lambert, W.; Hannibal, P.; Handrick, K. *Inorg. Chim. Acta* **1989**, *156*, 119.

(15) Lee, M. H.; Hwang, J.-E.; Kim, Y.; Kim, J.; Do, Y. *Organometallics* **1999**, *18*, 5124.

(16) Marsh, R. E.; Schaefer, W. P.; Coughlin, E. B.; Bercaw, J. E. *Acta Crystallogr.* **1992**, *C48*, 1773.

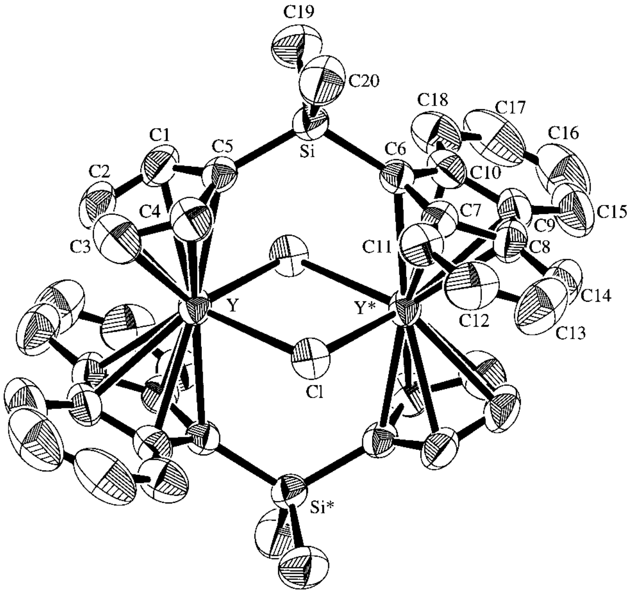

Figure 1. ORTEP diagram of $[Me_2Si(C_{13}H_8)(C_5H_4)Y(\mu\text{-}Cl)]_2{\cdot}1/2$toluene (**1**) with adopted atom numbering (most H atoms and toluene omitted for clarity).

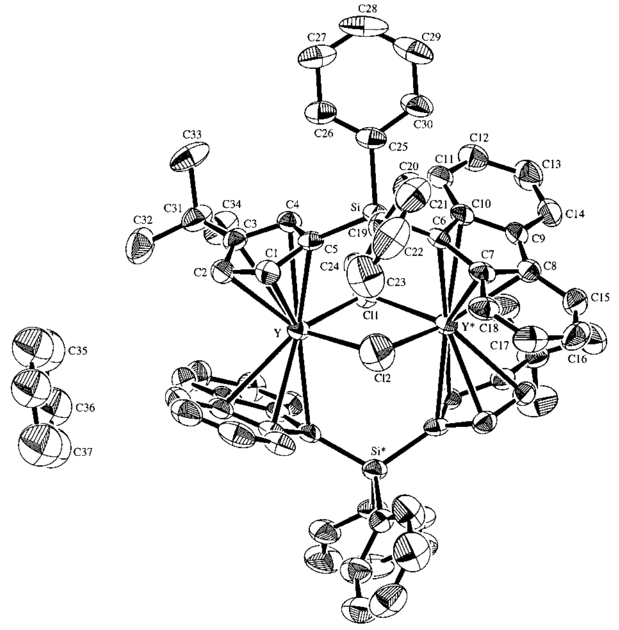

Figure 2. ORTEP diagram of $[Ph_2Si(C_{13}H_8)(^tBuC_5H_4)Y(\mu\text{-}Cl)]_2{\cdot}1/2$toluene (**5**) with adopted atom numbering (most H atoms and toluene omitted for clarity).

A characteristic feature of the bridging structure lies in the unusually widened C(5)−Si−C(6) angles (118.1(2)°, 116.1°) and the dihedral angle between the Cp ring plane (1) and Flu ring plane (2) (137.62°, 139.62°) in complexes **1** and **5**, respectively. The C(5)−Si−C(6) angle of **5** is 2° larger than that in the dimethylsilyene-bridged complex **1**. The larger dihedral angle in **5** between the Cp and Flu ring planes reflects the effect of the large ^{t}Bu-substituent on the Cp ring.

A remarkable difference exists between the C_s-symmetric complex **1** and the C_1-symmetric **5** in the bonding mode of the Ln atom to the two π-ring planes. In **1** the distances of Y−C(Cp, Flu ring) bonds ranging from 2.599 to 2.699 Å show the typical pattern of normal η^5-bonding fashion. However in complex **5** the Y−C(Cp, Flu ring) distances (2.604(6)−2.825(6) Å) no longer display the typical η^5-dispersion pattern. The ^{t}Bu−Cp ring in the complex **5** is coordinated to metal in both longer Y−C(2) and Y−C(3) bonds and shorter Y−C(ring) bonds at the unsubstituted side of the Cp ring. This phenomenon is also observed in various $Me_2SiCp''(R^*Cp)$-based compounds.[4a,c] The longer Y−C(8, 9, 10) (2.732(6)−2.825(6) Å) distances originated from the repulsive interaction between the ^{t}Bu group and the fluorenyl group which is on the other coordinated ligand.

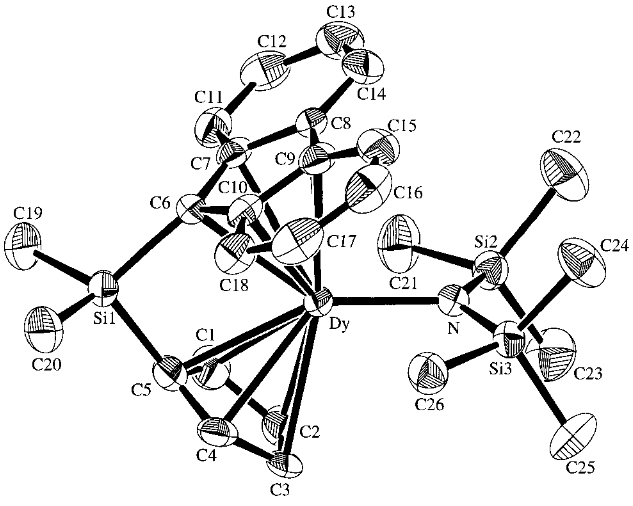

Figure 3. ORTEP diagram of $[Me_2Si(C_{13}H_8)(C_5H_4)]DyN(TMS)_2$ (**7**).

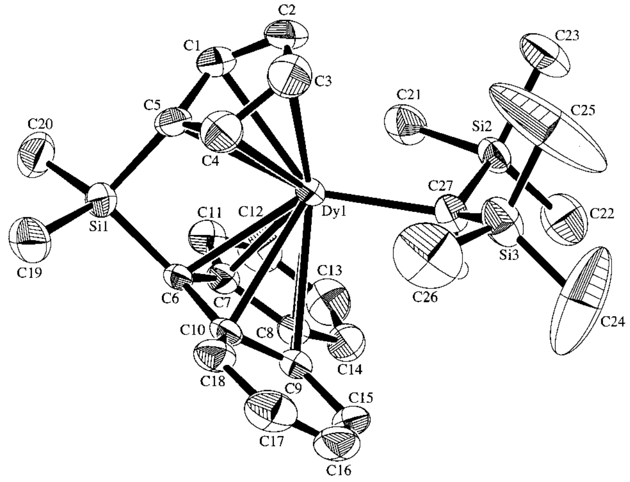

Figure 4. ORTEP diagram of $[Me_2Si(C_{13}H_8)(C_5H_4)]DyCH(TMS)_2$ (**8**).

The X-ray crystal structures display that in all of the amide and hydrocarbyl complexes one of the trimethylsilyl substituents approaches the Ln^{3+} center with an acute Ln−C_α−Si_β(1) angle, as observed commonly for $Cp'_2LnE(SiMe_3)_2$ (E = CH, N) derivatives. This geometry has been attributed to an interaction between the electron-deficient Ln^{3+} center and the electron-donating property of the Si−C bond.[17] In complex **7**, one of the Dy−N−Si angles is 106.8° and the other is 124.8°. This type of multicenter Ln−Me−Si interaction has been observed in numerous other organolanthanide amide complexes, for example, $(C_5Me_5)_2LnSm(TMS)_2$,[18] (*S*)-$[Me_2Si(C_5Me_4)((+)\text{-neomenthylCp})]LnN(TMS)_2$,[4c] (*S*)-

---

[17] Koga, N.; Morokuma, K. *J. Am. Chem. Soc.* **1988**, *110*, 108. (b) Tatsumi, K.; Nakamura, A. *J. Am. Chem. Soc.* **1987**, *109*, 3195.

[Me$_2$Si(C$_5$Me$_4$)((−)-menthylCp)]LnN(TMS)$_2$,[4a] and [Me$_2$Si(C$_5$Me$_4$)(C$_{13}$H$_8$)]YN(TMS)$_2$,[15] with the two Ln−N−Si$_\beta$ angles ranging from 103.6(6)° to 109.4(3)° (for ∠Ln−N−Si$_\beta$(1)) and from 121.5(5)° to 132.0(7)° (for ∠Ln−N−Si$_\beta$(2)). The short Dy−CH$_3$ contact (2.901(8) Å) is an apparent intermolecular γ-agostic Me−Ln interaction. The mode of this interaction is reflected at the different angles between N−Dy−C(2) (93.0(2)°) and N−Dy−C(3) (98.7(2)°). In the hydrocarbyl complex **8**, the two Dy−C(27)−Si angles (96.8(3)° and 129.8(5)°) resemble those observed in hydrocarbyl complexes (C$_5$Me$_5$)Y(OAr)CH(TMS)$_2$,[19] [Me$_2$Si(C$_5$H$_5$)(C$_5$Me$_4$)]LuCH(TMS)$_2$,[20] (*R*/*S*)-[Me$_2$Si(C$_5$Me$_4$)((+)-(neomenthylCp))YCH(TMS)$_2$,[4c] and [Me$_2$Si(C$_5$Me$_4$)(^{t}BuN)SmCH(TMS)$_2$,[21] with the two Ln−C$_\alpha$−Si$_\beta$ angles ranging from 92.2(6)° to 101.6(4)° for ∠Ln−C$_\alpha$−Si$_\beta$(1) and from 126.3(8)° to 134.5(9)° for ∠Ln−C$_\alpha$−Si$_\beta$(2). The equal distances of the central metal atom Ln to the two hydrogen H atoms on the γ-methyl group (2.72, 2.50, and 2.61 Å in complexes **7**, **8**, **9**, respectively) further demonstrate that there is a $^\beta$Si−Me−metal not a ($^\gamma$C)H−metal interaction. The longer Dy−H(37) (2.71 Å) distance and wider Dy−C(27)−H(37) (100.2(9)°) angle show that no ($^\alpha$C)H−metal interaction exists in the hydrocarbyl complex **8**.

There also exist some significant differences between the corresponding CH(TMS)$_2$ complexes and the amide complexes. The Dy−N (2.207(5) Å) bond distance is shorter than the corresponding distances for the other crystallographically characterized amides (e.g., for Cp′SmN(TMS)$_2$ (Sm−N = 2.301(3) Å), for Cp$_2$′YN(TMS)$_2$ (Y−N = 2.274(5) Å)). This shorter Ln−N distance should originate from the strong donation of the lone pair electron on nitrogen to the electron-deficient lanthanide metal center. The longer Dy−C(27) (2.364(9) Å) distance compared with the Dy−N distance appears to increase the agostic interactions between the Dy^{3+} and the Si−C bond, reflecting the longer bond length of Dy−C(21) (2.756 Å) in **8** and shorter Dy−C(26) (2.901 Å) in the N(TMS)$_2$ complex **7**.

The remarkable difference of these amide and hydrocarbyl complexes with their chloride precursor **1** is the increased strain around the central metal atom. This effect is caused by the bridged Si atom: it “pinches” the Cp and Flu rings and this effect is reflected in the acute dihedral angle between the Cp and Flu planes and smaller angle between the two C$_{\text{bridgehead}}$−Si− C$_{\text{bridgehead}}$ when compared with those observed in the bridging dimeric chloride **1**. For example in complex **7**, the two angles are 99.7(3)° and 65.87°, respectively. The bonding mode of the Dy atom with the fluorenyl ring fragments (Dy−C(ring), 2.618(9)−2.843(6) Å) might be described as being partially slipped toward η^3- from η^5-mode. The Dy−C(Cp ring) distances ranging from 2.615(6) to 2.657(6) Å are very uniform, indicating that the Cp ring is bonded to the Dy atom in the typical η^5-mode.

Polymerization of MMA. To examine the catalytic ability of compounds **7**, **8**, **9**, and **10** toward polar monomers, polymerization of MMA has been examined. Polymerization of MMA was performed in toluene solution, and after a fixed time the product was quenched with acidified methanol. Triad microstructure analysis of the polymer was carried out using ^{1}H NMR spectra. Results are summarized in Table 6.[21,22] All of these C_s-symmetric complexes show comparably high initiating activity (60−100%) and high syndiotacticity (60−83%). These results are very different from those reported by

Table 4. Selected Angles and Bonds for Complex 8

Bond Lengths (Å)			
Dy−C(27)	2.364(9)	Dy−Si(2)	3.148(3)
Dy−C(21)	2.756(10)	Dy−C(1)	2.589(10)
Dy−C(2)	2.66(1)	Dy−C(3)	2.69(1)
Dy−C(4)	2.619(10)	Dy−C(5)	2.604(9)
Dy−C(6)	2.592(8)	Dy−C(7)	2.662(8)
Dy−C(8)	2.816(8)	Dy−C(9)	2.830(9)
Dy−C(10)	2.666(8)	Si(2)−C(21)	1.898(10)
Si(2)−C(27)	1.818(9)	Si(3)−C(27)	1.840(8)
Si(2)−C(26)	1.88(2)	Dy−H(21)	2.50
Dy−H(37)	2.71	Dy−H(20)	3.68
Dy−H(19)	2.50		
Bond Angles (deg)			
Dy−C(27)−H(37)	100.2(9)	Dy−C(27)−Si(2)	96.8(5)
Dy−C(27)−Si(3)	129.8(5)	C(5)−Si(1)−C(9)	99.8(4)
C(19)−Si(1)−C(20)	108.2(5)	C(2)−Dy−C(27)	102.8(4)
C(3)−Dy−C(27)	93.7(3)	Si(2)−C(27)−Si(3)	123.5(5)
Dihedral Angle (deg)			
planes (1) and (2)		66.83	

Table 5. Selected Angles and Bonds for Complexes 7 and 9

	7	9
Bond Lengths (Å)		
Ln−N	2.207(5)	2.194(4)
Ln−C(21)	3.569(8)	3.667(7)
Ln−C(26)	2.901(8)	2.834(5)
Ln−Si(1)	3.407(2)	3.382(2)
Ln−Si(2)	3.469(2)	3.504(2)
Ln−Si(3)	3.152(2)	3.106(2)
Si(3)−C(26)	1.899(7)	1.896(5)
Si(3)−N	1.701(6)	1.697(4)
Si(2)−C(21)	1.861(9)	1.868(7)
Si(2)−N	1.699(5)	1.705(4)
Ln−C(1)	2.630(7)	2.596(6)
Ln−C(2)	2.657(8)	2.652(6)
Ln−C(3)	2.657(7)	2.647(5)
Ln−C(4)	2.615(7)	2.599(5)
Ln−C(5)	2.633(7)	2.603(4)
Ln−C(6)	2.618(6)	2.604(5)
Ln−C(7)	2.712(6)	2.670(5)
Ln−C(8)	2.843(6)	2.815(5)
Ln−C(9)	2.829(7)	2.816(5)
Ln−C(10)	2.675(6)	2.685(5)
Ln−H(35)	2.72	2.60
Ln−H(36)	2.71	2.61
Ln−H(37)	3.88	3.78
Bond Angles (deg)		
Si(2)−N−Si(3)	128.3(3)	127.1(2)
Ln−N−Si(3)	106.8(2)	105.2(2)
Ln−N−Si(2)	124.8(3)	127.6(2)
C(5)−Si(1)−C(6)	99.7(3)	99.5(2)
C(19)−Si(1)−C(20)	107.8(4)	107.7(3)
N−Ln−C(2)	93.0(2)	90.9(2)
N−Ln−C(3)	98.7(2)	98.2(2)
Dihedral Angle (deg)		
planes (1) and (2)	65.87	65.26

---

(18) Evans, W. J.; Keyer, R. A.; Ziller, J. W. *Organometallics* **1993**, *12*, 2618.

(19) Klooster, W. T.; Brammer, L.; Schaverien, C. J.; Budzelaar, P. H. M. *J. Am. Chem. Soc.* **1999**, *121*, 1381.

(20) Stern, D.; Sabat, M.; Marks, T. J. *J. Am. Chem. Soc.* **1990**, *112*, 9558.

(21) Tian, S.; Arredondo, V. M.; Stern, C. L.; Marks, T. J. *Organometallics* **1999**, *18*, 2568.

(22) Molecular weights and molecular weight distibutions for entry 4: $M_w(\times 10^4)$, 255.8 and 6.66; M_w/M_n, 2.802 and 1.490. For entry 6: $M_w(\times 10^4)$, 268.1 and 9.5; M_w/M_n, 1.472 and 1.577. For entry 9: $M_w(\times 10^4)$, 260.2 and 13.4; M_w/M_n, 1.290 and 2.441. For entry 10: only one peak, $M_w(\times 10^4)$, 6.8; M_w/M_n, 1.215.

Table 6. Data for the Polymerization of Methyl Methacrylate[a]

entry	catalyst	t_p (h)	T_p (°C)	conversn (%)	stereochem (%) rr	rm	mm
1	**7**	1	20	80.5	61	31	8
2	**7**	1	0	81.7	64	27	9
3	**7**	0.5	−20	98.2	59	26	4
4	**7**	0.5	−78	90.1	73	21	6
5	**7**	1	−95	100	80	20	0
6	**8**	1	20	100	60	33	7
7	**8**	0.5	0	88.6	59	34	7
8	**8**	1	−78	61.4	52	36	12
9	**9**	2	0	67.5	67	26	7
10	**9**	0.5	−78	100	82	18	0
11	**9**	1	−95	82.7	83	17	0
12	**10**	0.5	0	100	56	29	15
13	**10**	0.5	−78	48.3	68	26	4
14[b]	**9**	3	12	56.3	55		
15[c]	**9**	3	12	28.5	60		

[a] Reaction conditions: Initiator connection, 0.5 mol % monomer; solvent, toluene; Solv/[M_0] = 1 Vol/Vol. [b] Solvent, THF; Solv/[M_0] = 2 Vol/Vol. [c] Solvent, DME; Solv/[M_0] = 2 Vol/Vol.

Youngkyn and co-workers in 1999.[15] They used one of the Si-bridged C_s-symmetric amide complexes, [$Me_2Si(C_5Me_4)(Flu)$]$YN(TMS)_2$, as catalyst, and they obtained the iso-rich (56−58%) poly(MMA) in very low yield (4.2−10.4%). Yasuda has also reported one of the C-bridged alkyl complexes, [$Me_2C(2,7\text{-}^tBu_2\text{-}Flu)(Cp)$]$YCH(TMS)_2$,[23] inducing syn-rich polymerization of MMA (75−78%). T. J. Marks et al. reported the polymerziation of MMA using chiral C_1-symmetric rare-earth metal complexes.[6] It is likely that the stereoregularity varies with subtle difference in steric bulkiness between the complexes. From the results we can see that the slightly different R groups, when R = $N(TMS)_2$ and R = $CH(TMS)_2$, have obviously different activity. When lowering the temperature, the conversion and stereoregulation for the polymerization by amide complexes increased, while those by hydrocarbyls decreased. It can also be seen that erbium complexes have higher stereoselectivity than the dysprosium in this case.

Solvent effect has also been tested. We found that the stereoselectivity of poly(MMA) still remained syn-rich (about 50−60%) in THF or DME if **9** was used as an initiator (entries 14 and 15 in Table 6).

Molecular weights and molecular weight distributions of the polymers were determined by GPC in THF using standard polystyrene. We found that some polymer cannot be dissolved in THF or cannot pass through the columns of GPC. In almost all cases, GPC shows a bimodal pattern. One has very large molecular weights (>10^6) with lower ratio, and the other peak is the main products with high molecular weights (>10^5) and narrow molecular weight distributions.

Conclusion

In summary, we have successfully synthesized a series of new silylene-bridged fluorenyl cyclopentadienyl *ansa*-lanthanocene complexes with C_s symmetry and characterized their structural features by X-ray diffraction studies. These C_s-symmetric organolanthanides can be efficient catalysts for the syndio-rich polymerization of methyl methacrylate. We assume that the ability of a catalyst to control the syndiospecific entrance of the monomer is strongly dependent on the different steric volume of two π-ring fragments via achiral C_s-symmetric organo-rare-earth complexes

Experimental Section

All operations involving organometallics were carried out under an inert atmosphere of argon using standard Schlenk techniques. THF, toluene, and *n*-hexane were distilled from Na−benzophenone ketyl under argon prior to use. Anhydrous lanthanide chlorides[23,24] and *n*-butyllithium were prepared according to the procedures in the literature, and the reactant fluorene was purchased from Aldrich. ($C_{13}H_8$)$Me_2Si(C_5H_4)Li_2$[10] was synthesized using the method described in the literature for related compounds. Methyl methacrylate was purified by distillation from CaH_2 followed by storage over activated molecular sieves (3 Å) and then vacuum transferred using a high-vacuum line prior to use. Mass spectra were recorded on a HP 5989A spectrometer (T = 50−400 °C, 1.3 kV). The solvent C_6D_6 was degassed and dried over a Na/K alloy. ^1H NMR was performed on a Bruker Am-300 (300 MHz) spectrometer. Elemental analyses were performed by the Analytical Laboratory of the Shanghai Institute of Organic Chemistry.

Synthesis of [$Me_2Si(C_5H_4)(C_{13}H_8)YCl$]$_2$ (1). A solution of [$Me_2Si(C_5H_4)(C_{13}H_8)$]$Li_2$ (0.06 M, 106 mL in Et_2O) was added dropwise to a stirred suspension of YCl_3 (1.024 g, 6.36 mmol) in 20 mL of THF at −78 °C under argon. The reaction mixture was then slowly warmed to room temperature and stirred for 2 days. The precipitate was filtered off. The solvent was removed in vacuo and extracted with 50 mL of toluene. The supernatant was decanted, concentrated slightly, and cooled for crystallization at −20 °C. The yellow crystals generated (558 mg, 21.4%) were dried and submitted for X-ray analysis. Anal. Calcd for $C_{54}H_{22}Si_2Cl_2Y_2$ (**1**): C, 61.84; H, 4.83. Found: C, 62.12; H, 4.92. ^1H NMR (300 MHz, C_6D_6): δ 8.06 (d, 2H, FLu), 7.89 (d, 2H, Flu), 7.30 (m, 4H, Flu), 6.18 (t, 2H, Cp), 5.80 (t, 2H, Cp), 0.52 (s, 6H, $SiMe_2$). EI mass spectrum (70 eV, 50−400 °C): *m/z* 820 (5.54, [M]$^+$), 663 (3.64, [M − YCl_2]$^+$), 497 (12.35, [M − YCl_2−Flu]$^+$), 410 (100, [M/2]$^+$), 374 (40.25, [M/2 − Cl]$^+$). FT-Raman (cm^{-1}): 3067(m), 1527(s), 1437(s), 1336(vs), 1209(s), 1004(m), 740(m), 660(m), 521(w).

Synthesis of [$Me_2Si(C_5H_4)(C_{13}H_8)LuCl$]$_2$ (2). A procedure similar to that for complex **1** was adopted for $LuCl_3$ (1.277 g, 4.54 mmol), affording **2** as a yellow crystalline product (354 mg, 15.6%). Anal. Calcd for $C_{54}H_{22}Si_2Cl_2Lu_2$ (**2**): C, 46.37; H, 3.48. Found: C, 46.19; H, 3.74. ^1H NMR (300 MHz, C_6D_6): δ 8.04 (d, 2H, FLu), 7.89 (d, 2H, Flu), 7.27 (t, 2H, Flu), 7.16 (t, 2H, Flu), 6.06 (t, 2H, Cp), 5.67 (t, 2H, Cp), 0.54 (s, 6H, $SiMe_2$). EI mass spectrum (70 eV, 50−400 °C): *m/z* 992 (16.71, [M]$^+$), 749 (2.21, [M − YCl_2]$^+$), 583(4.65, [M − YCl_2−Flu]$^+$), 496 (100, [M/2]$^+$), 461 (32.66, [M/2 − Cl]$^+$). FT-Raman (cm^{-1}): 3069(m), 1520(s), 1438(s), 1337(vs), 1209(s), 1170(m), 740(m), 660(m), 521(w), 419(m), 292(m).

Synthesis of [$Me_2Si(C_5H_4)(C_{13}H_8)ErCl$]$_2$ (3). A procedure similar to that for complex **1** was adopted for $ErCl_3$ (1.468 g, 5.35 mmol), affording **3** as a yellow crystalline product (500 mg, 19.2%). Anal. Calcd for $C_{54}H_{22}Si_2Cl_2Er_2$ (**3**): C, 52.26; H, 4.11. Found: C, 52.35; H, 4.22. EI mass spectrum (70 eV, 50−400 °C): *m/z* 974 (14.17, [M]$^+$), 947 (3.88, [M − Cl]$^+$), 743 (8.31, [M − YCl_2]$^+$), 575 (18.56, [M − YCl_2−Flu]$^+$), 487 (81.06, [M/2]$^+$), 453 (100, [M/2 − Cl]$^+$). FT-Raman (cm^{-1}): 3067(m), 1527(s), 1438(s), 1338(vs), 1322(s), 1209(s), 1167(m), 1006(m), 740(m), 660(m), 521(w), 420(m), 290(m).

Synthesis of [$Me_2Si(C_5H_4)(C_{13}H_8)DyCl$]$_2$ (4). A procedure similar to that for complex **1** was adopted for $DyCl_3$ (1.110 g, 4.13 mmol), affording **4** as a yellow crystalline product (297 mg, 14.8%). Anal. Calcd for $C_{54}H_{22}Si_2Cl_2Dy_2$ (**4**): C, 53.08; H,

---

[23] Yasuda, Y.; Ihara, E. *Macromol. Chem. Phys.*, **1995**, *196*, 2417. Until now no detailed description of the synthesis and structural features of this complex have been reported.

[24] Chapman, J. H.; Owen, L. N. *J. Chem. Soc.* 1950, 579.

4.816. Found: C, 54.50; H, 4.27. EI mass spectrum (70 eV, 50−400 °C): *m/z* 970 (1.00, $[M]^+$), 4.85 (2.35, $[M/2]^+$), 450 (2.21, $[M/2 - Cl]^+$).

Synthesis of $[Ph_2Si(t\text{-}BuC_5H_3)(C_{13}H_8)YCl]_2$ (5). A procedure similar to that for complex **1** was adopted for YCl_3 (1.10 g, 5.64 mmol), affording **5** as a yellow crystalline product (1.23 g, 37.1%). Anal. Calcd for $C_{74}H_{66}Si_2Cl_2Y_2$ (**5**): C, 70.70; H, 5.34. Found: C, 70.34; H, 5.57. ^1H NMR (300 MHz, C_6D_6): δ 7.2−8.2 (m, CH(Ar)), 5.6−6.3 (m, CHCp), 1.37 (s, CH(^{t}Bu)). EI mass spectrum (70 eV, 50−400 °C): *m/z* 554 (0.32, $[M/2 - Cl]^+$), 302 (100, $[FluCPh_2]^+$). FT-Raman (cm^{-1}): 3046(m), 1587(s), 1529(s), 1335(vs), 1210(s), 998(vs), 672(m), 523(w), 425(m), 252(m).

Synthesis of $[Ph_2Si(t\text{-}BuC_5H_3)(C_{13}H_8)DyCl]_2$ (6). A procedure similar to that for complex **1** was adopted for $DyCl_3$ (1.00 g, 3.72 mmol), affording **6** as a yellow crystalline product (1.76 g, 71.5%). Anal. Calcd for $C_{34}H_{30}SiCl_2Dy$ (**6**): C, 59.56; H, 4.38. Found: C, 59.66; H, 4.51. EI mass spectrum (70 eV, 50−400 °C): *m/z* 1099 (4.23, $[M - DyCl_2]^+$), 665 (60.89, $[M/2]^+$), 630 (17.59, $[M/2 - Cl]^+$), 614 (74.16, $[M/2 - Cl-Me]^+$), 302 (100, $[FluCPh_2]$).

Synthesis of $[Me_2Si(C_5H_4)(C_{13}H_8)]DyN(TMS)_2$ (7). A solution of $[Me_2Si(C_5H_4)(C_{13}H_8)]Li_2$ (0.038M, 5.69 mmol, 150 mL in Et_2O) was added dropwise to a stirred suspension of $DyCl_3$ (1.53 g, 5.69 mmol) in 20 mL of THF at −78 °C under argon. The reaction mixture was then slowly warmed to room temperature and stirred for 2 days. The solvent was removed in vacuo and replaced with toluene (100 mL). Next the mixture was cooled to −78 °C, and $KN(TMS)_2$ (1.05 g, 5.5 mmol) was added slowly. The reaction mixture was allowed to warm to room temperature for 1 day and then warmed to 60 °C and stirred for 1 day. The precipitate was filtered off. The solvent was decanted, concentrated slightly, and cooled overnight at −20 °C for crystallization. Orange crystals were formed, suitable for X-ray analysis (1.317 g, 39.3%). Anal. Calcd for $C_{26}H_{36}Si_3NDy$ (**7**): C, 51.20; H, 5.91; N, 2.30. Found: C, 50.71; H, 6.05; N, 2.67. EI mass spectrum (70 eV, 50−400 °C): *m/z* 610 (100, $[M]^+$), 594 (47.90, $[M - Me]^+$), 450 (75.55, $[M - N(TMS)_2]^+$), 146 (47.41, $[N(TMS)_2]^+$). FT-Raman (cm^{-1}): 3047(s), 2898(vs), 1526(m), 1322(m), 1009(m), 742(w), 655(w), 610(w), 518(w), 430(m), 377(m), 237(s).

Synthesis of $[Me_2Si(C_5H_4)(C_{13}H_8)]DyCH(TMS)_2$ (8). A procedure similar to that for complex **7** was adopted for $DyCl_3$ (1.42 g, 5.30 mmol) and $LiN(TMS)_2$ (1.03 g, 6.2 mmol), affording **8** as a yellow crystalline product (523 mg, 12.6%). Anal. Calcd for $C_{27}H_{37}Si_3Dy$ (**8**): C, 51.25; H, 5.91. Found: C, 47.90; H, 6.55. EI mass spectrum (70 eV, 50−400 °C): *m/z* 609 (1.29, $[M]^+$), 594 (7.51, $[M - Me]^+$), 450 (100, $[M - N(TMS)_2]^+$), 145 (30.38, $[CH(TMS)_2]^+$). FT-Raman (cm^{-1}): 3047(s), 2899(vs), 1531(m), 1322(s), 1210(m), 742(m), 657(m), 577(m), 520(w), 431(m), 378(m), 236(s).

Synthesis of $[Me_2Si(C_5H_4)(C_{13}H_8)]ErN(TMS)_2$ (9). A procedure similar to that for complex **7** was adopted for $ErCl_3$ (1.304 g, 4.76 mmol) and $KN(TMS)_2$ (1.08 g, 5.4 mmol), affording **9** as a yellow crystalline product (330 mg, 11.5%). Anal. Calcd for $C_{26}H_{36}Si_3NEr$ (**9**): C, 50.81; H, 5.86; N, 2.28. Found: C, 50.68; H, 6.03; N, 2.51. EI mass spectrum (70 eV, 50−400 °C): *m/z* 615 (18.30, $[M]^+$), 599 (9.31, $[M - Me]^+$), 453 (6.98, $[M - N(TMS)_2]^+$), 146 (100, $[N(TMS)_2]^+$). FT-Raman (cm^{-1}): 3040(m), 2899(m), 1527(s), 1324(vs), 1211(s), 743(m), 656(m), 614(m), 520(w), 410(m), 378(m), 240(s).

Synthesis of $[Me_2Si(C_5H_4)(C_{13}H_8)]ErCH(TMS)_2$ (10). A procedure similar to that for complex **7** was adopted for $ErCl_3$ (1.468 g, 5.35 mmol) and $LiCH(TMS)_2$ (1.03 g, 6.2 mmol), affording **10** as a yellow crystalline product (240 mg, 7.3%). Anal. Calcd for $C_{27}H_{37}Si_3Er$ (**10**): C, 52.85; H, 6.04. Found: C, 52.97; H, 6.01. EI mass spectrum (70 eV, 50−400 °C): *m/z* 613 (2.13, $[M]^+$), 598 (2.08, $[M - Me]^+$), 454 (100, $[M - N(TMS)_2]^+$), 145 (46.84, $[CH(TMS)_2]^+$). FT-Raman (cm^{-1}): 3048(m), 2896(m), 1530(s), 1324(vs), 1211(s), 742(m), 657(m), 578(m), 520(w), 431(m), 378(m), 239(s).

Polymerization of MMA. A solution of preweighted catalyst (0.5 mmol) in toluene was adjusted to a constant temperature using an external bath. Into the well-stirred solution was syringed 100 mmol of methyl methacrylate, and the reaction was continuously stirred for an appropriate period at that temperature. Polymerization was stopped by addition of the acidic methanol. The resulting precipitated PMMA was collected, washed with methanol several times, and dried in vacuo at 50 °C for 12 h.

X-ray Structure Determination. Single crystals were sealed in thin-walled glass capillaries under an atmosphere of argon. X-ray diffraction data were collected at a room temperature using the $\omega - 2\theta$ scan technique to a maximum 2θ value of 50.0°. The intensities of three representative reflection were measured after every 200 reflections. Over the course of data collection, the standards decreased by 0.9%. A linear correction factor was applied to the data to account for this phenomenon. The data were corrected for Lorentz and polarization effects. The structures were solved by heavy-atom Patterson methods and expanded using Fourier techniques. The non-hydrogen atoms were refined anisotropically. All calculations were performed using the teXsan crystallographic software package of Molecular Structure Corporation.

Acknowledgment. The authors are grateful to the National Nature Science Foundation of China and Shanghai-Hong Kong Joint Laboratory in Chemical Synthesis for their financial support.

Supporting Information Available: Tables of atomic coordination, thermal parameters, and interatomic distances and angles for complexes **1**, **5**, **7**, **8**, and **9**. This material is available free of charge via the Internet at http://pubs.acs.org.

OM000276F